Real-time Fluorescence Imaging with IR700 Signal for Monitoring the Therapeutic Effects of Near-infrared Photoimmunotherapy

Tadanobu NAGAYA[1)2)]

1) *Department of Endoscopic Department, Shinshu University School Hospital*
2) *Molecular Imaging Program, Center for Cancer Research, National Cancer Institute, National Institutes of Health*

Aim : Near-infrared photoimmunotherapy (NIR-PIT) is a new, highly selective tumor treatment that employs a NIR phthalocyanine dye, IRDye 700DX (IR700), conjugated to a monoclonal antibody (mAb). Although NIR light exposure leads to immediate, target-selective necrotic cell death, actual tumor shrinkage occurs several days afterwards. Therefore, it is difficult to detect the immediate therapeutic effects by measuring tumor size. This study investigated IR700 fluorescence changes by means of fluorescence endoscopy as a potential real-time biomarker for monitoring cytotoxic effects during NIR-PIT.

Methods : *In vivo* mouse experiments were conducted with a human epidermal growth factor receptor type 2-expressing, green fluorescence protein (GFP)-expressing, gastric cancer cell line (N87-GFP). IR700 as a photosensitizer was conjugated to trastuzumab. The effects of NIR-PIT were evaluated in a flank xenograft model as well as in a disseminated peritoneal cancer model by GFP and IR700 real-time fluorescence imaging. Fluorescence intensity was compared before and after NIR-PIT for calculations of relative decreasing of fluorescence intensity (DFI).

Results : Tumor growth was significantly reduced and survival was significantly improved in the IR700 DFI ≤ 25 % group compared with the IR700 DFI >25 % group in Pearl images ($p<0.05$) in the flank xenograft model. In the disseminated peritoneal cancer model, an effective NIR-PIT therapeutic response was observed in the IR700 DFI ≤50 % group on fluorescence endoscopy.

Conclusion : IR700 fluorescence signal decrease during NIR-PIT may be a potential immediate indicator of the therapeutic effects of mAb-IR700-based NIR-PIT prior to the onset of tumor shrinkage. *Shinshu Med J 73 : 383—397, 2025*

(Received for publication July 1, 2025 ; accepted in revised form August 7, 2025)

Key words : near-infrared photoimmunotherapy, IR700, fluorescence imaging, fluorescence endoscopy, molecular imaging ; cancer therapy

Abbreviations : ANOVA, one-way analysis of variance ; APC, antibody-photoabsorber conjugate ; CCD, color-charge-coupled device ; DFI, decreasing of fluorescence intensity ; EGFR, epidermal growth factor receptor ; GFP, green fluorescence protein ; H&E, hematoxylin and eosin ; IR700, IRDye 700DX ; mAb, monoclonal antibody ; NIR, near-infrared ; PIT, photoimmunotherapy ; ROI, region of interest ; tra, trastuzumab

I Introduction

Despite rapid advances in diagnostic and therapeutic procedures, cancer remains one of the most deadly diseases worldwide[1)]. Near-infrared photoimmunotherapy (NIR-PIT) is a newly developed cancer treatment that employs a targeted monoclonal antibody (mAb)-photoabsorber conjugate (APC)[2)]. After the antibody binds to the appropriate cell-surface antigen, a photo-

Corresponding author : Tadanobu Nagaya
Department of Endoscopic Department, Shinshu University School Hospital
3-1-1 Asahi, Matsumoto, Nagano 390-8621, Japan
E-mail : nagaya@shishu-u.ac.jp

activatable silica-phthalocyanine dye, IRDye 700DX (IR700), induces lethal damage to the cell membrane after NIR-light exposure. NIR-PIT is effective with a variety of different antibodies conjugated to the same IR700 dye[2)-6)]. A first-in-human phase 1 trial of epidermal growth factor receptor (EGFR)-targeted NIR-PIT in patients with inoperable head and neck cancer was initiated in 2015. In 2021, the Japanese Agency for Pharmaceuticals and Medical Devices conditionally approved NIR-PIT for the treatment of previously treated, recurrent head and neck squamous cell carcinoma[7)8)].

Although NIR-PIT induces rapid necrotic/immunogenic cell death *in vitro*[9)], the immediate *in vivo* assessment of cell death is challenging since morphological changes are slow to develop, requiring several days to become apparent[10)] ; time is needed for macrophages to enter, process, and leave the treated tumor. Real-time monitoring of the therapeutic effects of NIR-PIT is desired to ascertain if a NIR-PIT session has been effective and whether adjustments are needed, such as additional doses of light or the mAb-IR700 conjugate, higher light intensity, or a combination of those factors. Immediate feedback is especially important during surgical or interventional procedures under endoscopy. Real-time prediction of treatment response has significant implications for intraoperative or endoscopic treatment planning. During treatment immediate feedback enables identification of areas with insufficient therapeutic effect due to factors such as limited light penetration or uneven probe distribution. This information allows clinicians to promptly adjust irradiation parameters, such as increasing the dose, extending the illumination time, or selectively re-illuminating suboptimal regions, thereby enhancing the precision and efficacy of treatment. This approach may contribute to improved treatment outcomes, reduced overtreatment or undertreatment, and decreased need for repeated procedures. Therefore, novel methods that can be implemented prior to size measurements are needed to monitor the effects of NIR-PIT.

Fluorescence proteins are commonly used for visualizing and tracking cellular processes[11)12)]. An advantage of fluorescence proteins for *in vivo* monitoring is that they do not require extrinsic agent injections and can be measured in real time[13)-15)]. However, they require gene transfection of fluorescence proteins to cancer cells *in vivo*, which might face challenges for approval by regulatory agencies. Fluorescence dye-conjugated drugs have also been used for the real-time monitoring of drug location and activation[16)-18)]. In addition, *in vivo* tracking of the cancer therapeutic effects of several nanoparticles has recently been reported[19)-22)]. Despite the great strides made towards smart probes for traceable cancer therapy, it remains difficult to develop a single molecular probe that is able to simultaneously detect, image, and ablate cancer cells as well as predict therapeutic responses *in vivo*.

The present study sought to determine whether IR700 fluorescence changes could serve as a real-time biomarker for monitoring the therapeutic effects of NIR-PIT.

Ⅱ Materials and Methods

A Reagents

Water soluble, silica-phthalocyanine derivative, IR700 NHS ester was obtained from LI-COR Biosciences (Lincoln, NE, USA). Trastuzumab (tra), a 95 % humanized IgG_1 mAb directed against human EGFR type 2, was purchased from Genentech (South San Francisco, CA, USA). All other chemicals were of reagent grade.

B Synthesis of IR700-conjugated tra

The conjugation of dye with a mAb was performed according to a previous report[2)]. Briefly, tra (1.0 mg, 6.8 nmol) was incubated with IR700 NHS ester (60.2 μg, 30.8 nmol) in 0.1 M Na_2HPO_4 (pH 8.6) at room temperature for 1 hour. The mixture was purified with a Sephadex G25 column (PD-10 ; GE Healthcare, Piscataway, NJ, USA). Protein concentration was determined with Coomassie Plus protein assay kit (Thermo Fisher Scientific Inc, Rockford, IL, USA) by measuring the absorption at 595 nm with UV-Vis (8453 Value System ; Agilent Technologies, Santa Clara, CA, USA). The concentration of IR700 was measured by absorption at 689 nm with spectroscopy to confirm the number of fluorophore mole-

cules conjugated to each mAb. The synthesis was controlled so that an average of two IR700 molecules were bound to a single antibody (tra-IR700).

C Cell culture

N87-GFP cells stably expressing green fluorescence protein (GFP) were purchased from ANTI CANCER (San Diego, CA, USA). High GFP expression was confirmed in the absence of a selection agent after 10 passages. Cells were grown in RPMI 1640 (Life Technologies, Gaithersburg, MD, USA) supplemented with 10 % fetal bovine serum and 1 % penicillin/streptomycin (Life Technologies) in tissue culture flasks in a humidified incubator at 37 ℃ in an atmosphere of 95 % air and 5 % carbon dioxide.

D Animal model

All *in vivo* procedures were conducted in compliance with the Guide for the Care and Use of Laboratory Animal Resources from the 1996 United States National Research Council, and approved by the local Animal Care and Use Committee. Six- to eight-week-old female homozygote athymic nude mice were purchased from Charles River (NCI-Frederick, Frederick, MD, USA). During the procedure, mice were anesthetized using inhaled isoflurane and intraperitoneal injection of 1 mg of sodium pentobarbital (Nembutal Sodium Solution, Ovation Pharmaceuticals Inc., Deerfield, IL, USA). To determine tumor volume, the greatest longitudinal diameter (length) and the greatest transverse diameter (width) were measured with an external caliper. Tumor volumes based on caliper measurements were calculated using the following formula : tumor volume = length × width^2 × 0.5. Body weight was also recorded. The general health of mice was monitored daily, and tumor volumes were measured three times a week until the tumor volume reached 2000 mm^3, at which time the mice were euthanized by carbon dioxide gas inhalation. The presence of skin necrosis or toxicity attributable to the APC was also evaluated by carefully noting skin color, general health, weight loss, and loss of appetite.

E *In vivo* fluorescence imaging

In vivo fluorescence images were obtained using a Pearl Imager (LI-COR Biosciences, Lincoln, NB, USA) with a 700 nm fluorescence channel. A region of interest (ROI) was placed on the tumor, and the average IR700 signal fluorescence intensity was calculated for each ROI using Pearl Cam Software (LI-COR Biosciences). For GFP imaging, a Maestro Imager (CRi, Woburn, MA, USA) with a band-pass excitation filter from 445 to 490 nm and a long-pass emission blue filter >515 nm was used. The tunable emission filter was automatically increased in 10 nm increments from 515 to 580 nm at a constant exposure time (250 msec for *in vivo* imaging and 100 msec for *ex vivo* imaging). Spectral fluorescence images consisted of autofluorescence spectra and spectra from GFP, which were then unmixed from each other based on the characteristic spectral pattern of GFP using Maestro software (CRi). A ROI was placed on the tumor in GFP images for the measurement of average fluorescence intensity. Relative decreasing of fluorescence intensity (DFI) was calculated using the following equation : DFI = average fluorescence intensity of tumor after NIR-PIT / average fluorescence intensity of tumor before NIR-PIT × 100 %. Due to the large inter-individual variability in IR700-derived DFI after NIR-PIT at the standard 100 J/cm^2 dose in mice, we measured post-treatment DFI values in approximately 10 mice for each imaging modality and defined the cutoff based on the average values. For the Pearl imager, the mean post-treatment IR700 DFI was 26.08 %, and we therefore set the cutoff at 25 %. For fluorescence endoscopy, the mean DFI was 48.97 % , and the cutoff was set at 50 %.

F NIR-PIT for the N87-GFP flank model

Ten million N87-GFP cells were injected subcutaneously in the right dorsum of each mouse. Tumors were studied after reaching a volume of approximately 50 mm^3. Following NIR exposure with a red light-emitting diode of 670 to 710 nm in wavelength (L690-66-60 ; Marubeni America Co., Santa Clara, CA, USA) and power density of 50 mW/cm^2 as measured with an optical power meter (PM 100, Thorlabs, Newton, NJ, USA), the tumor-bearing mice were divided into three groups of at least 10 animals per group for the following treatments : (1) no treatment

(control) ; (2) 100 μg of tra-IR700 i.v. to which NIR light was administered at 100 J/cm^2 on day 1 and IR700 DFI was ＞25 % (NIR-PIT-1) ; and (3) 100 μg of tra-IR700 i.v. to which NIR light was administered at 100 J/cm^2 on day 1 and IR700 DFI was ≤25 % (NIR-PIT-2). Serial fluorescence images and white light images were obtained with a Pearl Imager for detecting IR700 fluorescence, and a Maestro Imager was employed to detect GFP.

G *In vivo* fluorescence endoscopy

A fluorescence endoscopy model BF TYPE MP60 bronchoscope (Olympus Medical Systems, Tokyo, Japan) of 2.0 mm in diameter with a single biopsy channel was inserted into the abdominal cavity through a small abdominal incision for insufflation. The surface of the peritoneum was visualized with white light and fluorescence imaging using a clinical endoscopic system (CLV-180, Olympus Medical Systems, Tokyo, Japan) equipped with multi-band excitation filters. Endoscopic images were obtained via a beam splitter, in which white light images were detected using a color-charge-coupled device (CCD) camera and fluorescence images were filtered by an emission filter (516 to 556 nm band-pass for GFP and 680 to 710 nm band-pass for IR700), and then captured with anCCD camera (Texas Instruments, Dallas, TX, USA). Real-time images of both the white light and fluorescence images were displayed side by side on a computer monitor and recorded. In order to compare fluorescence intensities during NIR-PIT, the distance between the tumor and endoscope head was maintained using biopsy forceps (FB-56D-1, Olympus Medical Systems, Tokyo, Japan) as a guide. Camera gain, exposure time, and binning for the fluorescence images were held constant throughout the study.

H *Ex vivo* histological analysis

Mice were euthanized with an overdose of carbon dioxide 6 hours after NIR-PIT for the N87-GFP flank model, then tumors were excised. Resected tumors were fixed for at least 24 hours with 10 % formalin. After paraffin-embedded sections at 10 μm were stained with hematoxylin and eosin (H&E), histological analysis was conducted using a fluorescence microscope (BX61 ; Olympus America, Inc., Melville, NY, USA).

I NIR-PIT for the N87-GFP disseminated peritoneal model

To generate the disseminated peritoneal cancer mouse model, ten million N87-GFP cells suspended in phosphate buffered saline (total 400 μL) were injected into the peritoneal cavity. Mice exhibited disseminated peritoneal cancer at 2 weeks after cell implantation and were injected intravenously with 100 μg of tra-IR700. One day afterwards, *in vivo* images were acquired with fluorescence endoscopy. Tumors of 2 to 3 mm in size were selected using biopsy forceps as a measure. After obtaining initial fluorescence images of the peritoneal surface, tumor-bearing mice were randomized into four groups of at least 10 animals per group for the following treatments : (1) NIR light administered at 20 J/cm^2 ; (2) NIR light administered at 50 J/cm^2 ; (3) NIR light administered at 100 J/cm^2 ; and (4) NIR light administered until IR700 DFI ≤50 % . Tumors were irradiated with a NIR laser emitting light at 685 to 695 nm in wavelength (BWF5-690-8-600-0.37 ; B&W TEK INC., Newark, DE, USA) through the skin. The output power density in mW/cm^2 was measured using an optical power meter (PM 100, Thorlabs). The abdomen of mice was externally exposed to NIR light from the ventral side, with the upper abdominal area shielded from light exposure by aluminum foil to prevent light exposure to liver. Real-time fluorescence images of the disseminated peritoneal cancers were repeatedly recorded immediately after NIR exposure and at 6 hours after NIR-PIT. The fluorescence measurement at 6 hours after NIR-PIT was included to explore the dynamics of IR700 and GFP fluorescence over time and to investigate whether a delayed signal change might provide additional information regarding treatment response. Image analysis was performed with ImageJ software (http://rsb.info.nih.gov/ij/). Circular ROIs were placed in the same regions to determine the fluorescence intensities.

J Histological analysis

Real-time tumor biopsies were performed through the fluorescence endoscope using biopsy forceps

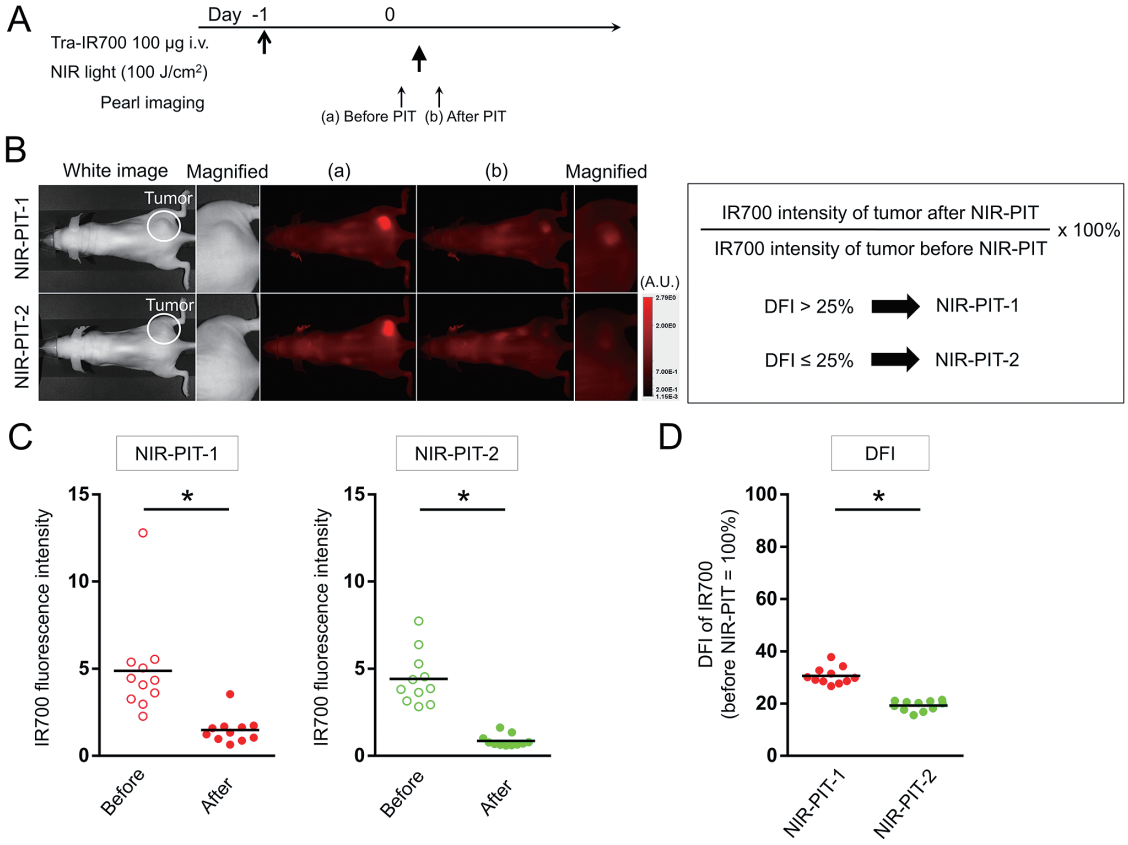

Fig. 1 *In vivo* characterization of NIR-PIT

(A) Treatment and imaging regimen of NIR-PIT. (B) Mice were divided into two groups according to the IR700 DFI after NIR-PIT. (C) Quantification of the IR700 fluorescence intensity of NIR-PIT-1 (left) and NIR-PIT-2 (right). The IR700 fluorescence signal of tumors was significantly decreased after NIR-PIT (n = 11, $^{*}p = 0.001$ for NIR-PIT-1 and $^{*}p < 0.0001$ for NIR-PIT-2, Student's *t*-test). (D) IR700 DFI in tumors. The IR700 DFI in the NIR-PIT-2 group was significantly lower than in the NIR-PIT-1 group (n = 11, $^{*}p < 0.001$, Student's *t*-test).

(FB-56D-1, Olympus Co., Tokyo, Japan) beginning at 6 hours after NIR-PIT for the N87-GFP disseminated peritoneal model. Mice were euthanized with an overdose of carbon dioxide afterwards. Biopsy specimens were fixed for at least 24 hours with 10 % formalin. After paraffin-embedded sections were stained with hematoxylin and eosin (H&E), post-NIR-PIT tissue analysis was conducted using a fluorescence microscope (BX61 ; Olympus America, Inc., Melville, NY, USA).

K Statistical analysis

Data are expressed as the mean ± standard error of the mean. Statistical analyses were carried out using GraphPad Prism version 7 (GraphPad Software, La Jolla, CA, USA). Student's *t*-test was employed to compare the fluorescence intensity of tumors. For multiple comparisons, one-way analysis of variance (ANOVA) followed by Bonferroni's correction for multiple comparisons was used. The cumulative probability of survival based on volume (2000 mm^3) was estimated for each group by Kaplan-Meier survival curve analysis, and the results were compared by means of the log-rank test. A *p*-value < 0.05 was considered to indicate a statistically significant difference.

Ⅲ Results

A *In vivo* characterization of NIR-PIT

The treatment regimen is shown in **Fig. 1A**. One day after the injection of tra-IR700, tumors showed high fluorescence intensity. Following exposure to 100 J/cm^2 of NIR light, the IR700 fluorescence signal of tumors decreased significantly due to dying cells

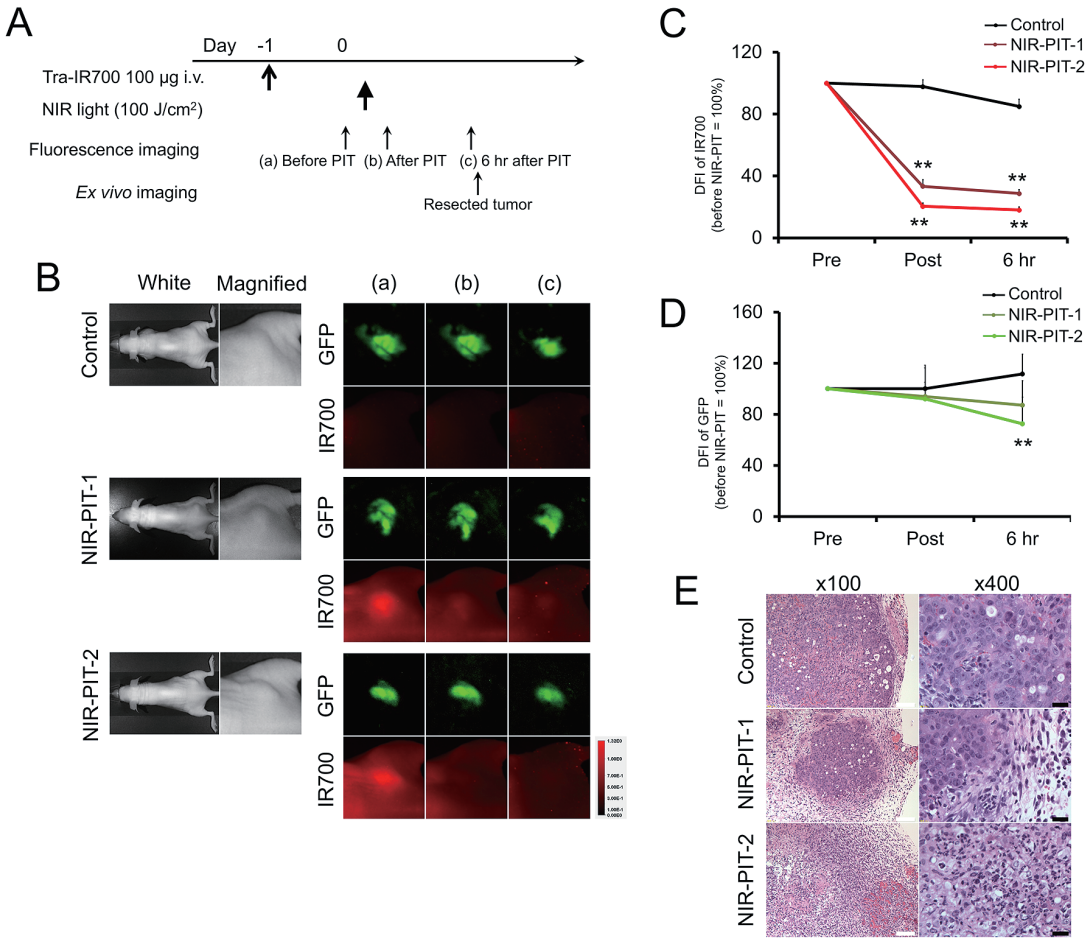

Fig. 2 *In vivo* and *ex vivo* imaging of N87-GFP tumors

(A) Treatment and imaging regimen. (B) *In vivo* fluorescence real-time imaging of tumor-bearing mice in response to NIR-PIT. Tumors treated by NIR-PIT showed a decreased IR700 fluorescence signal, while the GFP fluorescence signal did not change remarkably. (C) Quantification of IR700 DFI. The IR700 fluorescence signal of tumors was significantly decreased after NIR-PIT in both NIR-PIT-1 and NIR-PIT-2 tumors (n = 10, $^{**}p < 0.0001$, Student's *t*-test). (D) Quantification of GFP DFI. No significant differences were evident in DFI immediately after NIR-PIT and 6 hours after NIR-PIT-1 group, with the GFP fluorescence signal significantly decreased at 6 hours after NIR-PIT in NIR-PIT-2 tumors (n = 10, $^{**}p < 0.01$, Student's *t*-test). (E) Resected tumors stained with H&E. Several scattered clusters of damaged tumor cells were visible within a background of diffuse cellular necrosis and micro-hemorrhage after NIR-PIT. Necrotic damage was more intense and fewer tumor cells remained in NIR-PIT-2 tumors (white bar = 100 μm, black bar = 20 μm).

and partial photo-bleaching **(Fig. 1B)**. Mice were divided into two groups according to IR700 DFI after NIR-PIT : the NIR-PIT-1 group (IR700 DFI >25 %) and the NIR-PIT-2 group (IR700 DFI ≤25 %) **(Fig. 1B)**. The IR700 fluorescence intensity of tumors decreased significantly after NIR-PIT in both groups ($p = 0.001$ and $p < 0.0001$, respectively) **(Fig. 1C)**. The IR700 DFI in the NIR-PIT-2 group was significantly lower than in the NIR-PIT-1 group ($p < 0.0001$) **(Fig. 1D)**.

B *In vivo* and *ex vivo* imaging of N87-GFP tumors

The treatment and imaging regimen is summarized in **Fig. 2A**. In *in vivo* imaging, the IR700 fluorescence signal of tumors decreased significantly from dying cells and partial photo-bleaching immediately after exposure to 100 J/cm^2 of NIR light ($p < 0.0001$) **(Fig. 2B, C)**. On the other hand, the GFP signal did not change immediately after NIR exposure **(Fig. 2B, D)**. Six hours after NIR-PIT, the GFP signal in NIR-PIT-2 tumors was significantly lower than in control tumors ($p < 0.01$), with no significant

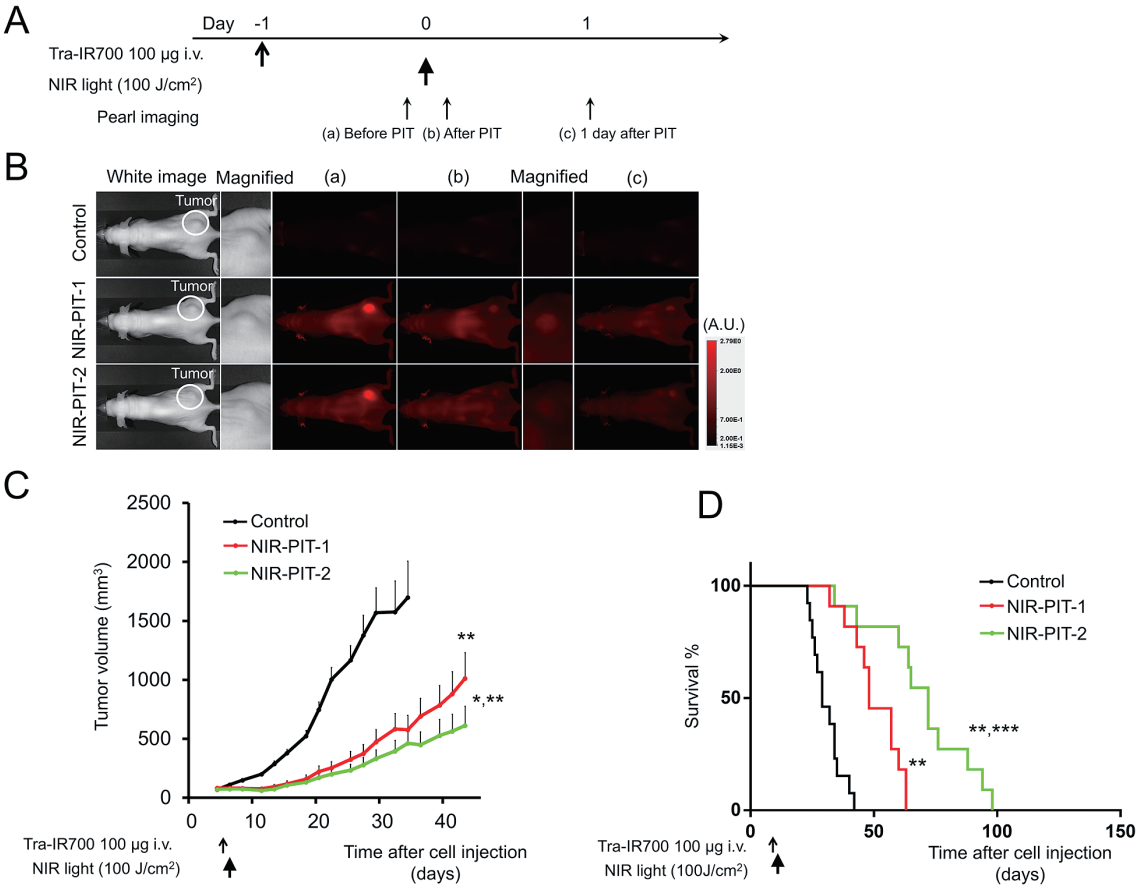

Fig. 3 *In vivo* NIR-PIT effects in the N87-GFP flank model

(A) Treatment and imaging regimen. (B) *In vivo* fluorescence real-time imaging of tumor-bearing mice in response to NIR-PIT. Tumors showed higher fluorescence intensity than those with no APC. Tumors treated by NIR-PIT exhibited decreasing IR700 fluorescence signal after NIR-PIT. (C) Tumor growth was significantly inhibited in both the NIR-PIT-1 and NIR-PIT-2 treatment groups compared with the control group ($^{**}p<0.01$ vs. control group, Bonferroni test with ANOVA). Tumor growth was also significantly reduced in the NIR-PIT-2 group versus the NIR-PIT-1 group (n≥10, $^{*}p<0.05$, Bonferroni test with ANOVA). (D) Significantly prolonged survival was observed in both the NIR-PIT-1 and NIR-PIT-2 treatment groups compared with the control group (n≥10, $^{**}p<0.01$, log-rank test). Survival was significantly more improved in the NIR-PIT-2 group than in the NIR-PIT-1 group (n≥10, $^{***}p<0.01$, log-rank test).

difference between the GFP signal in control and NIR-PIT-1 tumors **(Fig. 2D)**. Regarding *ex vivo* imaging, most of the IR700 fluorescence signal had disappeared at 6 hours after NIR-PIT in NIR-PIT-2 tumors, while the IR700 signal remained in NIR-PIT-1 tumors **(Fig. 2E)**. We observed no remarkable differences for the GFP signal **(Fig. 2E)**. Microscopic evaluation of treated tumors revealed diffuse necrosis and microhemorrhage, with scattered clusters of damaged tumor cells. Necrotic damage was more intense and fewer tumor cells remained in NIR-PIT-2 tumors **(Fig. 2F)**.

C *In vivo* NIR-PIT effect in the N87-GFP flank model

The treatment and imaging regimen is depicted in **Fig. 3A**. One day after injection of tra-IR700, tumors showed higher fluorescence intensity than those with no APC. Following exposure to 100 J/cm^2 of NIR light, the IR700 fluorescence signal decreased significantly in NIR-PIT-2 tumors but remained in NIR-PIT-1 tumors **(Fig. 3B)**. Tumor growth was significantly inhibited in both the NIR-PIT-1 and NIR-PIT-2 groups compared with the control group (both $p<0.01$) **(Fig. 3C)**, with significantly prolonged survival

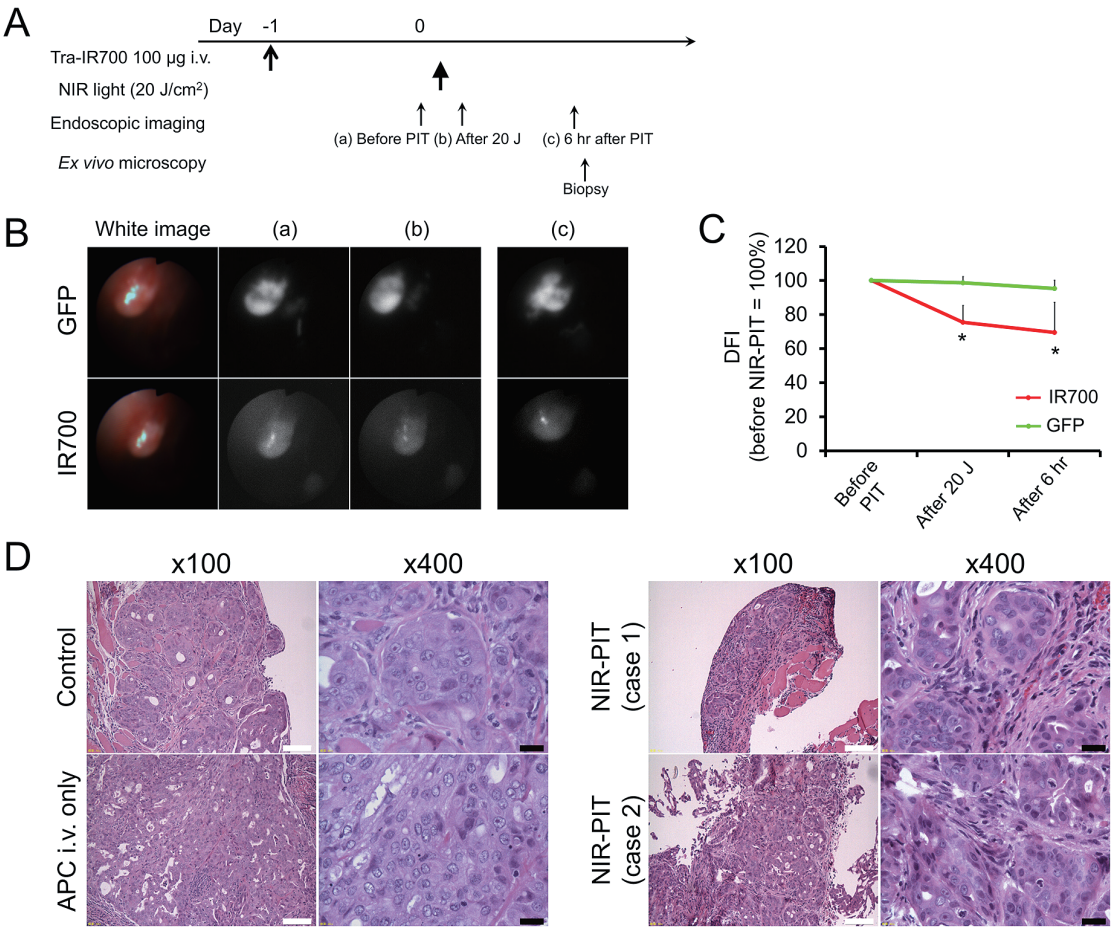

Fig. 4 Evaluation of NIR-PIT (20 J) effects on the disseminated peritoneal model

(A) Treatment and imaging regimen. (B) *In vivo* endoscopic imaging of the disseminated peritoneal model in response to NIR-PIT. The IR700 fluorescence signal coincided with GFP-positive foci. The IR700 fluorescence signal also showed tumor-specific accumulation with high tumor-to-background ratio. The IR700 fluorescence signal decreased immediately after NIR light exposure, while the GFP fluorescence signal did not change remarkably. (C) Quantification of both GFP and IR700 DFI. The IR700 fluorescence signal of tumors significantly decreased immediately after NIR-PIT compared with GFP fluorescence signal ($n=10$, $^{*}p<0.05$, Student's t-test). The IR700 DFI was approximately 70 % after 20 J/cm^2 of NIR light exposure. (D) Histological specimens of N87-GFP tumors stained with H&E. No obvious damage was observed in either control tumors or tumors at 6 hours after tra-IR700 injection without NIR light exposure (left). NIR-PIT-treated tumors showed necrosis and micro-hemorrhage with scattered clusters of damaged cancer cells. Undamaged cancer cells were evident as well (right) (white bar = 100 μm, black bar = 20 μm).

as well (both $p<0.01$ vs. control) **(Fig. 3D)**. Furthermore, tumor growth was significantly inhibited and survival was significantly longer in the NIR-PIT-2 group versus the NIR-PIT-1 group ($p<0.05$ for tumor growth and $p<0.01$ for survival) **(Fig. 3C, D)**. No skin necrosis or toxicity attributable to the APC was detected in any group.

D *In vivo* fluorescence endoscopic study in the N87-GFP disseminated peritoneal model

1 20 J/cm^2 of NIR-PIT

The treatment and imaging procedure is shown in **Fig. 4A**. After tra-IR700 injection, the implanted intraperitoneal disseminated tumors demonstrated fluorescence commensurate with IR700, which co-localized with GFP **(Fig. 4B)**. The IR700 fluorescence signal decreased immediately after 20 J/cm^2 of NIR-PIT. In contrast, the GFP fluorescence signal did not change remarkably ($p<0.05$ at the point of after 20J and after 6 hr) **(Fig. 4B, C)**. The IR700 DFI was approximately 70 % after 20 J/cm^2 of NIR-PIT. In

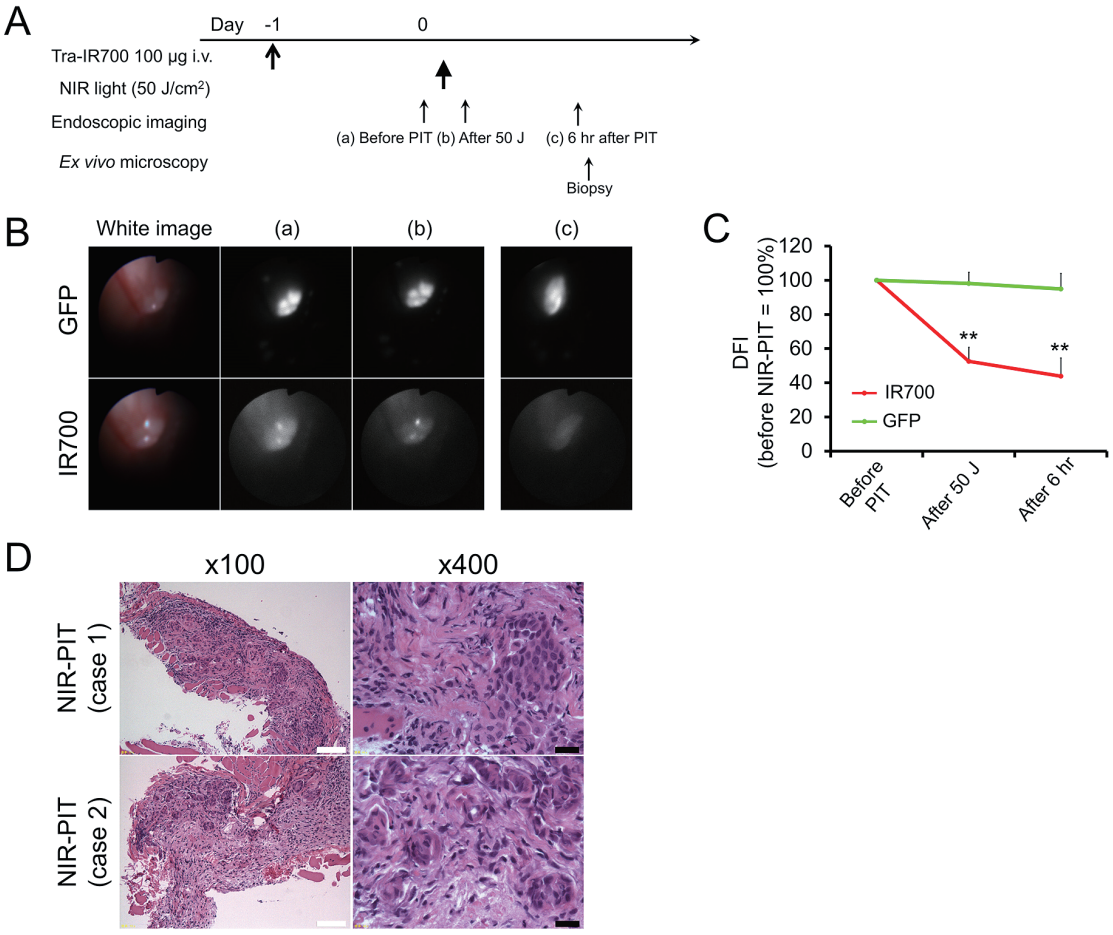

Fig. 5 Evaluation of NIR-PIT (50 J) effects on the disseminated peritoneal model

(A) Treatment and imaging regimen. (B) *In vivo* endoscopic imaging of the disseminated peritoneal model in response to NIR-PIT. The IR700 fluorescence signal decreased immediately after NIR light exposure, while GFP fluorescence signal did not change demonstrably. (C) Quantification of GFP and IR700 fluorescence intensity. The IR700 fluorescence signal of tumors significantly decreased immediately after NIR-PIT compared with GFP fluorescence signal (n = 10, $^{**}p < 0.01$, Student's t-test). The IR700 DFI was approximately 50 % after 50 J/cm^2 of NIR light exposure. (D) Histological specimens of N87-GFP tumors stained with H&E. Several scattered clusters of damaged tumor cells are seen within a background of diffuse cellular necrosis and micro-hemorrhage. Almost all cancer cells were damaged by NIR-PIT (white bar = 100 μm, black bar = 20 μm).

H&E-stained histological specimens, no obvious damage was observed in control or APC i.v.-only tumors. NIR-PIT-treated tumors exhibited necrosis and micro-hemorrhage with scattered clusters of damaged cancer cells, although undamaged cancer cells were also detectable **(Fig. 4D)**.

2 50 J/cm^2 of NIR-PIT

The treatment and imaging regimen is presented in **Fig. 5A**. The GFP fluorescence signal of tumors did not change demonstrably after NIR-PIT. On the other hand, the IR700 fluorescence signal decreased immediately after 50 J/cm^2 of NIR-PIT ($p < 0.01$ at the point of after 50J and after 6 hr) **(Fig. 5B, C)**. The IR700 DFI was approximately 50 % following 50 J/cm^2 of NIR light exposure. Pathological analysis revealed necrosis and micro-hemorrhage ; however, cancer cells showing no damage were also observed **(Fig.5D)**.

3 100 J/cm^2 of NIR-PIT

The treatment and imaging protocol is shown in **Fig. 6A**. The IR700 fluorescence signal decreased immediately after 100 J/cm^2 of NIR-PIT, while the

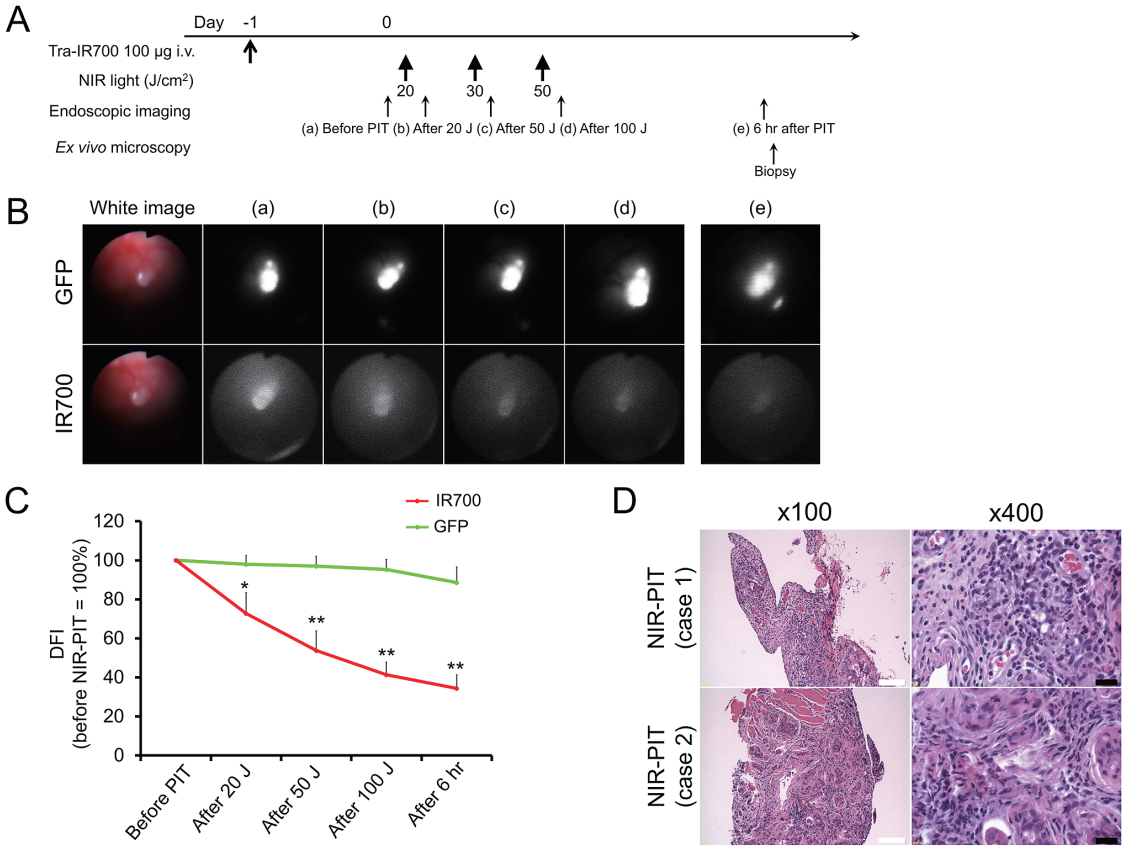

Fig. 6 Evaluation of NIR-PIT (100 J) effects on the disseminated peritoneal model

(A) Treatment and imaging regimen. (B) *In vivo* endoscopic imaging of the disseminated peritoneal model in response to NIR-PIT. The IR700 fluorescence signal decreased immediately after NIR light exposure, while the GFP fluorescence signal of tumors was slightly decreased at 6 hours after NIR light exposure. (C) Quantification of GFP and IR700 fluorescence intensity. The IR700 fluorescence intensity of tumors significantly decreased immediately after NIR-PIT compared with GFP fluorescence signal (n = 10, $^{*}p<0.05$, $^{**}p<0.01$, Student's t-test). The IR700 DFI was approximately 40 % after 100 J/cm^2 of NIR light exposure. (D) Histological specimens of N87-GFP tumors stained with H&E. Virtually all cancer cells were damaged by NIR-PIT (white bar = 100 μm, black bar = 20 μm).

GFP signal of tumors had decreased slightly at 6 hours after NIR-PIT ($p<0.05$ at the point of after 20J, $p<0.01$ at the point of after 50J, after 100J and after 6 hr) **(Fig. 6B, C)**. The IR700 DFI was approximately 40 % following 100 J/cm^2 of NIR-PIT. In histological analysis, virtually all cancer cells were damaged by NIR-PIT **(Fig. 6D)**.

4 Light dose adjustment of NIR-PIT

The above results indicated that approximately < 50 % of IR700 DFI in fluorescence endoscopic imaging was needed to obtain a sufficient therapeutic effect. Thus, we adjusted the NIR light dose until IR700 DFI reached ≤50 % **(Fig. 7A, B)**. An average of 48.4 J of NIR light was needed to attain IR700 DFI ≤50 % **(Fig. 7C)**. Histological analysis showed that almost all cancer cells were damaged as a result of NIR-PIT with IR700 DFI ≤50 % **(Fig. 7C)**.

Ⅳ Discussion

This study revealed that during NIR-PIT, the IR700 fluorescence signal of tumors continuously decreased as shown in **Fig. 7C**. Histological experiments demonstrated that sufficient IR700 DFI of < 25 % in Pearl images or <50 % on fluorescence endoscopy corresponded to a strong therapeutic effect of NIR-PIT. After exposure to sufficient NIR light energy, the IR700-conjugated drug produced immediate cell membrane damage that was associated with a signif-

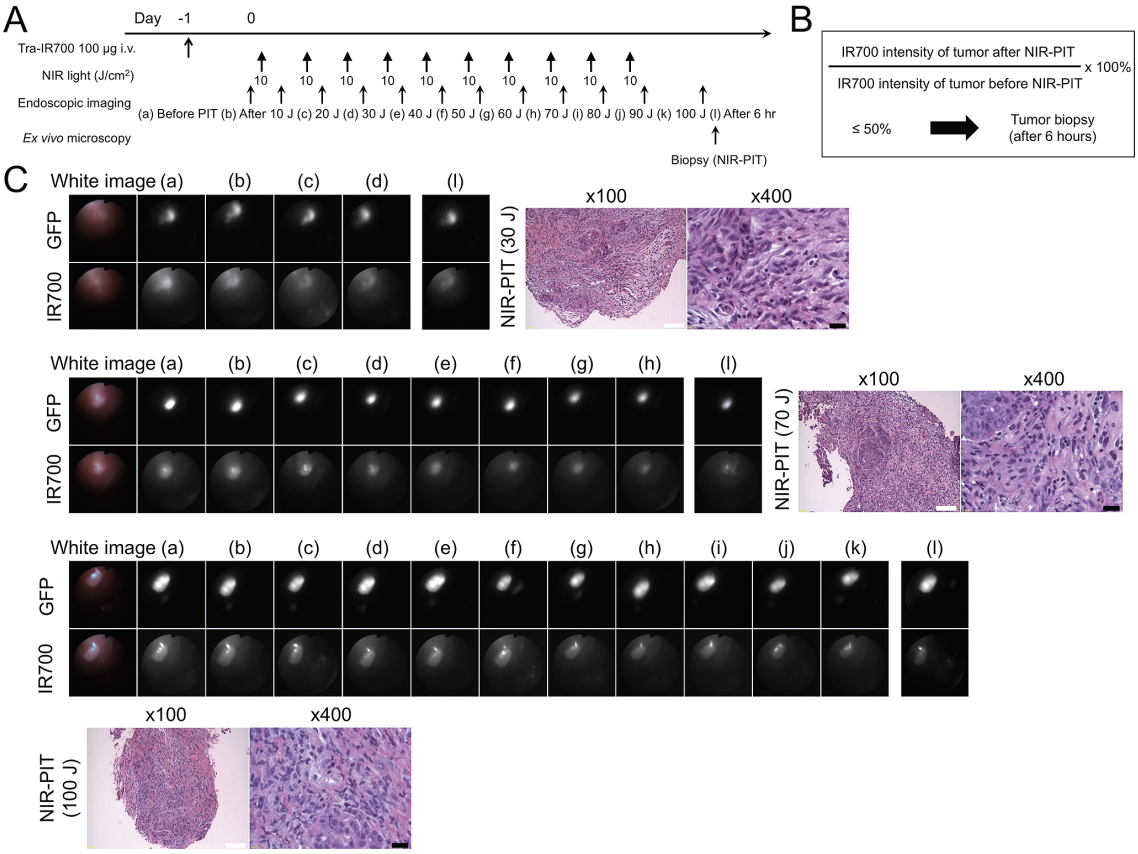

Fig. 7 Evaluation of adjusted NIR-PIT effects on the disseminated peritoneal model

(A) Treatment and imaging regimen. (B) NIR light was administered until IR700 DFI ≤50 %. (C) *In vivo* endoscopic imaging of the disseminated peritoneal model in response to NIR-PIT. The IR700 fluorescence signal decreased immediately after NIR light exposure, while the GFP fluorescence signal of tumors did not change remarkably. Histological specimens of N87-GFP tumors stained with H&E (white bar = 100 μm, black bar = 20 μm). Almost all cancer cells were damaged by NIR-PIT regardless of NIR light dose.

icant reduction in the IR700 signal. These findings suggested that a sufficient decrease in the IR700 fluorescence signal represented a potential imaging biomarker for evaluating the acute therapeutic effects of NIR-PIT.

Uptake and retention of the IR700 conjugate in target tumors is especially important in the setting of NIR-PIT. This study demonstrated that tra-IR700 could be effectively delivered to intraperitoneal tumors after intravenous injection, with tumors clearly detectable on fluorescence endoscopy as shown in **Fig. 2 to 5.** These results indicated that IR700-conjugated mAbs might have a practical clinical application during endoscopic procedures. From the photophysical point of view, the endoscope can minimize light scattering and absorbance caused by overlapping tissue, resulting in more precise lesion depiction. The development of a mini-endoscope mimicking laparoscopy may enable intraperitoneal fluorescence imaging and is the most likely method by which NIR-PIT can be administered and monitored in humans. Fluorescence endoscopic imaging renders it possible to simultaneously monitor APC accumulation by IR700 fluorescence as well as NIR-PIT effect via decreasing IR700 fluorescence signal. From the pharmacokinetic perspective, as IR700 conjugation minimally alters the pharmacokinetics of the antibody, these APCs show specific binding to target cells with minimal attachment to non-target cells[2)4)5)23)-25)]. APCs can be synthesized from virtually any antibody. Therefore, real-time NIR-PIT monitoring may be applied to numerous tumors without additional procedures.

Tumor size is considered a delayed indicator of tumor response, yet is still used clinically, however, changes in tumor size typically become evident only after several days to weeks following therapy. A more immediate readout of cell death is desired, especially in surgical or endoscopic procedures where it is preferable to complete treatments in a single session. Real-time IR700 fluorescence provides immediate feedback during or shortly after treatment, allowing for on-the-spot assessment of therapeutic effect. In particular, real-time evaluation using IR700 fluorescence could be especially valuable in endoscopic or laparoscopic procedures, where direct intraoperative visualization and decision-making are possible. By monitoring IR700 fluorescence intensity during endoscopic or laparoscopic procedures, clinicians may identify areas that have not received sufficient NIR light exposure and adjust the irradiation dose accordingly. This enables more precise and balanced treatment delivery, potentially minimizing under- or over-treatment during NIR-PIT.

Fluorescence proteins are a potential alternative for monitoring tumor growth *in vivo*[26)27)]. However, fluorescence imaging using such proteins may be more suited for longitudinally monitoring the effects of phototherapy[28)29)]. While most apoptic cell death preserves the cell membrane and retains the fluorescence proteins, making fluorescence insensitive to cell death[30)31)], the sudden rupture of cell membranes in NIR-PIT, which clearly represents necrotic cell death, results in the extrusion of cytoplasmic fluorescence proteins and a relatively rapid readout of cell death within seconds after NIR light exposure[24)]. In contrast, significant differences were not detected until 6 hours after NIR light exposure for the GFP fluorescence signal in this study. Fluorescence proteins also require gene transfection that would likely only be useful in pre-clinical studies. Considering that IR700-conjugated drugs require only intravenous injection, real-time IR700 fluorescence imaging appears better suited for detecting acute changes in treated tumors versus fluorescence proteins.

Concerning other cancer therapeutic monitoring methods, positron emission tomography, magnetic resonance imaging, and fluorescence lifetime imaging are also useful imaging biomarkers for detecting early changes after NIR-PIT before alterations in tumor size became evident[32)-34)]. Compared with those methods, optical imaging techniques do not require the use of radioactive materials. Furthermore, the imaging system and scanning process for fluorescence imaging employ low-cost, easy-to-use, portable equipment. The optical imaging probes for fluorescence imaging are usually less expensive and much easier to generate than radiotracers as well. Optical imaging also facilitates multicolor imaging by means of fluorophores with different emission wavelengths[35)]. Even compared with radiotracers, real-time fluorescence imaging is a promising technique for a broad range of clinical settings.

Advanced-stage gastric cancer is associated with a poor prognosis, with a 5-year survival rate below 5 % in metastatic cases. Standard treatment includes chemotherapy, and in patients with HER2 overexpression, the addition of trastuzumab has shown clinical benefit. However, the overall outcome remains poor, underscoring the need for novel therapeutic strategies[36)37)]. NIR-PIT is expected to be effective against HER2-positive gastric cancer, and its clinical application using endoscopic approaches is highly anticipated. In such settings, the ability to monitor treatment response in real time during the procedure would further enhance its therapeutic utility, so we established a peritoneal dissemination model using a HER2-positive gastric cancer cell line and conducted the present study.

Lastly, the disadvantages of optical imaging for *in vivo* NIR-PIT monitoring must be acknowledged as well. One issue is that optical signals have limited tissue penetration depth. Fluorescence imaging allows efficient photon tissue penetration with minimal intratissue light scattering. However, optical imaging remains inherently limited in terms of detecting relatively superficial tumors, such as breast cancer, thyroid gland tumor, and skin carcinoma. Recent advances have adapted optical imaging for endoscopic use or image-guided surgery[38)] to enable access to deep tissues inside the body. When consid-

ering NIR-PIT of the peritoneal cavity, direct exposure of NIR light deep into the patient is necessary using either direct illumination during surgery or using fibro-optic diffusers via endoscopes, laparoscopes, or inserted needles. Applying NIR light to the treatment of exposed residual tumors after surgical resection might be another way to incorporate NIR-PIT into patient management. In such cases, IR700 conjugates would be able to simultaneously detect tumors, treat cancer cells, and predict the therapeutic response in real-time.

V Conclusion

Real-time optical imaging of the IR700 fluorescence signal is a potential biomarker for immediately assessing the therapeutic effects of NIR-PIT with a mAb-IR700 conjugate during surgical or endoscopic procedures, even before morphological changes become evident.

Acknowledgments

This research was supported by the Intramural Research Program of the National Institutes of Health, National Cancer Institute, Center for Cancer Research.

Disclosure of potential conflicts of interest

None declared.

References

1) Siegel R, Naishadham D, Jemal A : Cancer statistics, 2013. CA Cancer J Clin 63 : 11-30, 2013
2) Mitsunaga M, Ogawa M, Kosaka N, Rosenblum LT, Choyke PL, Kobayashi H : Cancer cell-selective in vivo near infrared photoimmunotherapy targeting specific membrane molecules. Nat Med 17 : 1685-1691, 2011
3) Hanaoka H, Nagaya T, Sato K, et al : Glypican-3 targeted human heavy chain antibody as a drug carrier for hepatocellular carcinoma therapy. Mol Pharm 12 : 2151-2157, 2015
4) Nagaya T, Nakamura Y, Sato K, Harada T, Choyke PL, Kobayashi H : Near infrared photoimmunotherapy of B-cell lymphoma. Mol Oncol 10 : 1404-1414, 2016
5) Nagaya T, Nakamura Y, Sato K, et al : Near infrared photoimmunotherapy with an anti-mesothelin antibody. Oncotarget 7 : 23361-23369, 2016
6) Watanabe R, Hanaoka H, Sato K, et al : Photoimmunotherapy targeting prostate-specific membrane antigen : are antibody fragments as effective as antibodies ? J Nucl Med 56 : 140-144, 2015
7) Matsuoka K, Sato M, Sato K : Hurdles for the wide implementation of photoimmunotherapy. Immunotherapy 13 : 1427-1438, 2021
8) Yamada M, Matsuoka K, Sato M, Sato K : Recent Advances in Localized Immunomodulation Technology : Application of NIR-PIT toward Clinical Control of the Local Immune System. Pharmaceutics 15 : 561, 2023
9) Ogawa M, Tomita Y, Nakamura Y, et al : Immunogenic cancer cell death selectively induced by near infrared photoimmunotherapy initiates host tumor immunity. Oncotarget 8 : 10425-10436, 2017
10) Mitsunaga M, Nakajima T, Sano K, Kramer-Marek G, Choyke PL, Kobayashi H : Immediate in vivo target-specific cancer cell death after near infrared photoimmunotherapy. BMC Cancer 12 : 345, 2012
11) Hoffman R : Green fluorescent protein imaging of tumour growth, metastasis, and angiogenesis in mouse models. Lancet Oncol 3 : 546-556, 2002
12) Hoffman RM : The multiple uses of fluorescent proteins to visualize cancer in vivo. Nat Rev Cancer 5 : 796-806, 2005
13) Caysa H, Hoffmann S, Luetzkendorf J, et al : Monitoring of xenograft tumor growth and response to chemotherapy by non-invasive in vivo multispectral fluorescence imaging. PLoS One 7 : e47927, 2012
14) Cordero AB, Kwon Y, Hua X, Godwin AK : In vivo imaging and therapeutic treatments in an orthotopic mouse model of ovarian cancer. J Vis Exp 42 : 2125, 2010
15) Ma T, Liu H, Sun X, et al : Serial in vivo imaging using a fluorescence probe allows identification of tumor early response to cetuximab immunotherapy. Mol Pharm 12 : 10-17, 2015

16) Bhuniya S, Maiti S, Kim EJ, et al : An activatable theranostic for targeted cancer therapy and imaging. Angew Chem Int Ed Engl 53 : 4469–4474, 2014
17) Santra S, Kaittanis C, Santiesteban OJ, Perez JM : Cell-specific, activatable, and theranostic prodrug for dual-targeted cancer imaging and therapy. J Am Chem Soc 133 : 16680–16688, 2011
18) Yuan Y, Chen Y, Tang BZ, Liu B : A targeted theranostic platinum (IV) prodrug containing a luminogen with aggregation-induced emission (AIE) characteristics for in situ monitoring of drug activation. Chem Commun (Camb) 50 : 3868–3870, 2014
19) Ali T, Nakajima T, Sano K, Sato K, Choyke PL, Kobayashi H : Dynamic fluorescent imaging with indocyanine green for monitoring the therapeutic effects of photoimmunotherapy. Contrast Media Mol Imaging 9 : 276–282, 2014
20) Min Y, Li J, Liu F, Yeow EK, Xing B : Near-infrared light-mediated photoactivation of a platinum antitumor prodrug and simultaneous cellular apoptosis imaging by upconversion-luminescent nanoparticles. Angew Chem Int Ed Engl 53 : 1012–1016, 2014
21) Tian J, Ding L, Ju H, et al : A multifunctional nanomicelle for real-time targeted imaging and precise near-infrared cancer therapy. Angew Chem Int Ed Engl 53 : 9544–9549, 2014
22) Yuan Y, Kwok RT, Tang BZ, Liu B : Smart Probe for Tracing Cancer Therapy : Selective Cancer Cell Detection, Image-Guided Ablation, and Prediction of Therapeutic Response In Situ. Small 11 : 4682–4690, 2015
23) Mitsunaga M, Nakajima T, Sano K, Choyke PL, Kobayashi H : Near-infrared theranostic photoimmunotherapy (PIT) : repeated exposure of light enhances the effect of immunoconjugate. Bioconjug Chem 23 : 604–609, 2012
24) Sato K, Choyke PL, Kobayashi H : Photoimmunotherapy of gastric cancer peritoneal carcinomatosis in a mouse model. PLoS One 9 : e113276, 2014
25) Sato K, Nagaya T, Choyke PL, Kobayashi H : Near infrared photoimmunotherapy in the treatment of pleural disseminated NSCLC : preclinical experience. Theranostics 5 : 698–709, 2015
26) Hoffman RM, Yang M : Whole-body imaging with fluorescent proteins. Nat Protoc 1 : 1429–1438, 2006
27) Yamamoto N, Jiang P, Yang M, et al : Cellular dynamics visualized in live cells in vitro and in vivo by differential dual-color nuclear-cytoplasmic fluorescent-protein expression. Cancer Res 64 : 4251–4256, 2004
28) Hoffman RM, Yang M : Subcellular imaging in the live mouse. Nat Protoc 1 : 775–782, 2006
29) Jiang P, Yamauchi K, Yang M, et al : Tumor cells genetically labeled with GFP in the nucleus and RFP in the cytoplasm for imaging cellular dynamics. Cell Cycle 5 : 1198–1201, 2006
30) Vermes I, Haanen C, Reutelingsperger C : Flow cytometry of apoptotic cell death. J Immunol Methods 243 : 167–190, 2000
31) Walsh GM, Dewson G, Wardlaw AJ, Levi-Schaffer F, Moqbel R : A comparative study of different methods for the assessment of apoptosis and necrosis in human eosinophils. J Immunol Methods 217 : 153–163, 1998
32) Nakajima T, Sano K, Mitsunaga M, Choyke PL, Kobayashi H : Real-time monitoring of in vivo acute necrotic cancer cell death induced by near infrared photoimmunotherapy using fluorescence lifetime imaging. Cancer Res 72 : 4622–4628, 2012
33) Nakamura Y, Bernardo M, Nagaya T, et al : MR imaging biomarkers for evaluating therapeutic effects shortly after near infrared photoimmunotherapy. Oncotarget 7 : 17254–17264, 2016
34) Sano K, Mitsunaga M, Nakajima T, Choyke PL, Kobayashi H : Acute cytotoxic effects of photoimmunotherapy assessed by 18F-FDG PET. J Nucl Med 54 : 770–775, 2013
35) Schaafsma BE, Mieog JS, Hutteman M, et al : The clinical use of indocyanine green as a near-infrared fluorescent contrast agent for image-guided oncologic surgery. J Surg Oncol 104 : 323–332, 2011
36) Bang YJ, Van Cutsem E, Feyereislova A, et al : Trastuzumab in combination with chemotherapy versus chemotherapy alone for treatment of HER2-positive advanced gastric or gastro-oesophageal junction cancer (ToGA) : a phase 3, open-label, randomised controlled trial. Lancet 376 : 687–697, 2010

37) Lordick F, Carneiro F, Cascinu S, et al : Gastric cancer : ESMO Clinical Practice Guideline for diagnosis, treatment and follow-up. Ann Oncol 33 : 1005-1020, 2022

38) van Dam GM, Themelis G, Crane LM, et al : Intraoperative tumor-specific fluorescence imaging in ovarian cancer by folate receptor-alpha targeting : first in-human results. Nat Med 17 : 1315-1319, 2011

(2025. 7. 1 received ; 2025. 8. 7 accepted)